Measurement of hypoxia in the lung in IPF: An F-MISO PET CT Study

*Joanna C Porter[1] *Thida Win[2], Kjell Erlandsson[3], Francesco Fraioli[3], Alaleh Rashidnasab[3], Beverley Holman[3], Balaji Ganeshan[3], Nicholas J Screaton[4], Toby M Maher[6], Raymond Endozo[3], John Hoath[3], Robert I Shortman[3], Elise Emond[3], Kris Thielemans[3], Brian F Hutton[3], Pauline T Lukey[7], Franklin Aigbirhio[8], Saif Khan[9], Manuel Rodriguez-Justo[9], Ashley M Groves[3]
* Joint First Authors

[1]CITR, UCL and Interstitial Lung Disease Centre, UCLH, London UK
[2]Respiratory Medicine, Lister Hospital, Stevenage, UK.
[3]Institute of Nuclear Medicine, UCL/H, London, UK.
[4]Radiology Department, Papworth Hospital, Papworth Everard, UK
[5]Interstitial Lung Disease Unit, Royal Brompton Hospital, London, UK
[6] Royal Brompton Hospital, Sydney Street, London. UK
[7]Target to Treatment Consulting Ltd, Stevenage Bioscience Catalyst, Stevenage, UK
[8]Wolfson Brain Imaging Centre, University Cambridge. Cambridge, UK
[9]Department of Histopathology, UCLH, London UK

INTRODUCTION

Idiopathic pulmonary fibrosis (IPF) is a chronic fibrosing lung disease, with an incidence of ~1/10,000 per year, and a poor prognosis with limited treatments [1]. The role of hypoxia in disease progression is unclear.

Although it is plausible that the IPF lung is hypoxic, much of the evidence is indirect. To our knowledge this is the first study to explore the potential role of the hypoxia tracer fluoromisonidazole (F-MISO) in understanding pathomechanisms in IPF. We present the data from 10 IPF patients.

The hypoxia response is regulated by the hypoxia inducible transcription factors (HIF) which regulate gene expression. There is up-regulation of hypoxia-related markers~~, including HIF-1α, TGF β, and pathways~~ in IPF lung [2]; in some reports CA-IX, a cellular signal of hypoxia, alongside HIF-1α and 2α has been found in the epithelium overlying fibroblastic foci in IPF. Levels of lactic acid are high in IPF lung supporting the concept of a hypoxic microenvironment [3].

Nitroimidazoles are electron affinic molecules that accumulate in hypoxic cells in culture and *in vivo*. These compounds, including F-MISO, are metabolized by intracellular nitroreductases, and at low oxygen levels serve as competing electron acceptors. They are reduced and form covalent bonds to macromolecules, thus becoming biochemically trapped within these hypoxic yet metabolically active cells [4]. A quantitative, although non-linear, inverse relationship between nitroimidazole binding and oxygen concentration has been described [5]. PET imaging of tissue hypoxia (pO2 ≤ 3 mm Hg) using ^{18}F-labeled fluoromisonidazole (FMISO) is the most frequent use of a nitroimidazole imaging agent [6].

A better understanding of the degree and extent of hypoxia in individual patients with IPF may offer novel approaches for treatment, allow stratification of patients for clinic trials, and detect treatment response. Using the hypoxic reporter fluoromisonidazole (F-MISO), we have a tool to detect hypoxia in IPF with molecular imaging.

METHODS

10 patients with IPF were consented and underwent ^{18}F-MISO PET/CT following ethical approval Each patient had been discussed in an ILD MDT that had reached a consensus diagnosis of IPF, based on clinical, radiological and pathological (when available) findings. In all indeterminate cases, a biopsy showed histological UIP. Biopsy proven lung cancer patients that had undergone ^{18}F-MISO PET/CT were included as controls.

PET/CT data were acquired on the same PET CT (VCT PET/64-detector CT instrument, GE Healthcare Technology, WI). "Combined CTs" [7], were used for attenuation and air fraction correction (AFC)[7,8].

$1cm^3$ spherical VOIs were placed on fibrotic (F) and normal appearing control (C) regions distant from fibrosis, in each IPF patient; and around tumour or radiological/ non-emphysematous lung in patients with lung cancer. Average pulmonary uptake (SUV_{mean}) and tissue-to-blood ratio (TBR) values of ^{18}F-FMISO were quantified in each ROI on static PET images obtained at 220mins post injection. The ROIs were propagated to dynamic PET frames to obtain time-activity-curves (TACs). An additional ROI (~0.6 cm^3) was drawn on the ascending aorta for blood TAC and to obtain an image derived input function.

Kinetic analysis was performed using software developed in-house in MATLAB (MathWorks, Natick, MA, USA) using a combination of two different approaches: compartmental modelling and graphical analysis for irreversible tracers (Patlak plot). An irreversible 3-tissue compartment model was used and a parameter estimating the trapping of tracer in the hypoxic cells calculated. This parameter is independent of blood volume, blood flow and air fraction, and is therefore appropriate to use in the IPF lung.

Immunohistochemistry was performed using the Bond-Max system (Leica Biosystems Ltd., Newcastle) using 4-μm FFPE sections. HIF1α (clone: EP1215y), HIF2α (Rabbit polyclonal) and CA-IX (clone TH22). Staining was scored as previously described [9] and samples of adenocarcinoma of the lung were used as positive controls.

RESULTS

Characteristics of the patients are shown in Table 1. All patients had peripheral oxygen saturations of >94% at rest with the exception of patient 1 who was at 84%. In contrast to the signal detected in a lung cancer patient there was very little uptake of ^{18}F-MISO in any of the 10 IPF patients. On quantification following air fraction correction (AFC), there was no significant difference in either SUV_{mean} or TBR ratios between F and C regions on static ^{18}F-FMISO scans SUV_{mean}: C=1.6±0.18, F=1.55±0.19, p=0.36; TBR: C=1.25±0.14, F=1.19±0.12, p=0.11. The dynamic ^{18}F-FMISO analysis showed that tracer uptake measured by the trapping rate ($k_5{}^*$) was much less variable than influx rate K_i, with a mean value close to zero for both the normal and fibrotic lung in IPF. $k_5{}^*$:C=-2.1·10^{-4}±1.8·10^{-3} min^{-1}, F=-8.5·10^{-5}±1.4·10^{-3} min^{-1}, p=0.81.

Four IPF patients underwent lung biopsy after PET scanning. Immunohistochemistry showed variable and limited epithelial HIF-1α and HIF-2α expression, particularly over areas of fibroblastic foci, and at levels lower than seen in a lung adenocarcinoma control biopsy. There was no CAIX detected in any of the IPF biopsies.

DISCUSSION

Following validated methodology to correct for confounding effects, we showed no evidence for widespread hypoxia with PET/CT F-MISO imaging in the IPF cases despite detection of low levels of HIF-1α and HIF-2α on immunohistochemistry.

In terms of the static data analysis, a TBR threshold of 1.48 has been used to identify hypoxic tissue [10]. Using these criteria, almost all IPF ROIs would be classified as non-hypoxic. For dynamic analysis of ^{18}F-FMISO data the k_5^* parameter, which reflects the trapping of the tracer, was zero for C and FROIs.

Assuming that tracer is effectively delivered to the fibrotic areas, our results indicate a surprising lack of ^{18}F-MISO uptake in IPF. One caveat is that our studies, scans and biopsies, were performed with patients at rest and ignoring the potential for exercise-induced hypoxia.

In summary, immunohistochemistry reveals some markers of hypoxia in IPF however there may not be sufficient cells that are both hypoxic and viable to allow detection by ^{18}F-MISO. This contrasts with the situation in cancer, in which hypoxia is a recognised feature, detectable both on IHC and with ^{18}F-MISO. We conclude that hypoxia in the IPF lung is too mild and diffuse, compared with the marked focal hypoxia in the centre of a tumour, to detect with this imaging technique. We propose that further studies are needed to understand the optimal method to measure hypoxia in this devastating disease.

REFERENCES

1. Gross TJ, Hunninghake GW. Idiopathic pulmonary fibrosis. N Engl J Med. 2001;345:517–25.
2. Landi C, Bargagli E, Carleo A, Bianchi L, Gagliardi A, Prasse A, et al. A system biology study of BALF from patients affected by idiopathic pulmonary fibrosis (IPF) and healthy controls. Proteomics Clin Appl. 2014;8:932–50.
3. Kottmann RM, Kulkarni AA, Smolnycki KA, Lyda E, Dahanayake T, Salibi R, et al. Lactic acid is elevated in idiopathic pulmonary fibrosis and induces myofibroblast differentiation via pH-dependent activation of transforming growth factor-β. Am J Respir Crit Care Med. 2012;186:740–51.
4. Chapman JD, Franko AJ, Sharplin J. A marker for hypoxic cells in tumours with potential clinical applicability. Br J Cancer. Nature Publishing Group; 1981;43:546–50.
5. Rasey JS, Grunbaum Z, Magee S, Nelson NJ, Olive PL, Durand RE, et al. Characterization of radiolabeled fluoromisonidazole as a probe for hypoxic cells. Radiat Res. 1987;111:292–304.
6. Rajendran JG, Mankoff DA, O'Sullivan F, Peterson LM, Schwartz DL, Conrad EU, et al. Hypoxia and glucose metabolism in malignant tumors: evaluation by [18F]fluoromisonidazole and [18F]fluorodeoxyglucose positron emission tomography imaging. Clin Cancer Res. 2004;10:2245–52.

7. Holman BF, Cuplov V, Millner L, Hutton BF, Maher TM, Groves AM, et al. Improved correction for the tissue fraction effect in lung PET/CT imaging. Phys Med Biol. 2015;60:7387–402.

8. Lambrou T, Groves AM, Erlandsson K, Screaton N, Endozo R, Win T, et al. The importance of correction for tissue fraction effects in lung PET: preliminary findings. Eur J Nucl Med Mol Imaging. 2011;38:2238–46.

9. Groves AM, Shastry M, Rodriguez-Justo M, Malhotra A, Endozo R, Davidson T, et al. ^{18}F-FDG PET and biomarkers for tumour angiogenesis in early breast cancer. Eur J Nucl Med Mol Imaging. 2011;38:46–52.

10. Asano A, Ueda S, Kuji I, Yamane T, Takeuchi H, Hirokawa E, et al. Intracellular hypoxia measured by 18F-fluoromisonidazole positron emission tomography has prognostic impact in patients with estrogen receptor-positive breast cancer. Breast Cancer Research. 2018;20:78.

Table 1

| Patient	Age	Sex	FVC (% pred)	TLCO (% pred)	Lung biopsy	CA-IX Intensity	HIF-1α Intensity	HIF-2α Intensity	GAP Score
1 IPF	64	M	43.2	25.1	Yes	Negative	Negative	++	6 points stage III
2 IPF	74	M	98.1	41.4	No	-	-	-	4 points stage II
3 IPF	51	F	99	79.0	Yes	Negative	+	++	0 points stage I
4 IPF	68	M	62.8	32.2	No	-	-	-	6 points stage III
5 IPF	66	F	102	45.8	Yes	Negative	Negative	-	3 points stage I
6 IPF	85	F	78	44.0	No	-	-	-	3 points stage I
7 IPF	63	M	84.3	48.4	Yes	Negative	Negative	++	3 points stage I
8 IPF	69	F	104	-	No	-	-	-	4 points stage II
9 IPF	61	M	82	65.0	No	-	-	-	2 points stage I
10 IPF	72	M	84	49.0	No	-	-	-	4 points stage II
11 Lung cancer	N/A	N/A	N/A	N/A	Yes	+	+	+++	N/A
12 Lung cancer	N/A	N/A	N/A	N/A	Yes	++	+++	++	N/A

Figure
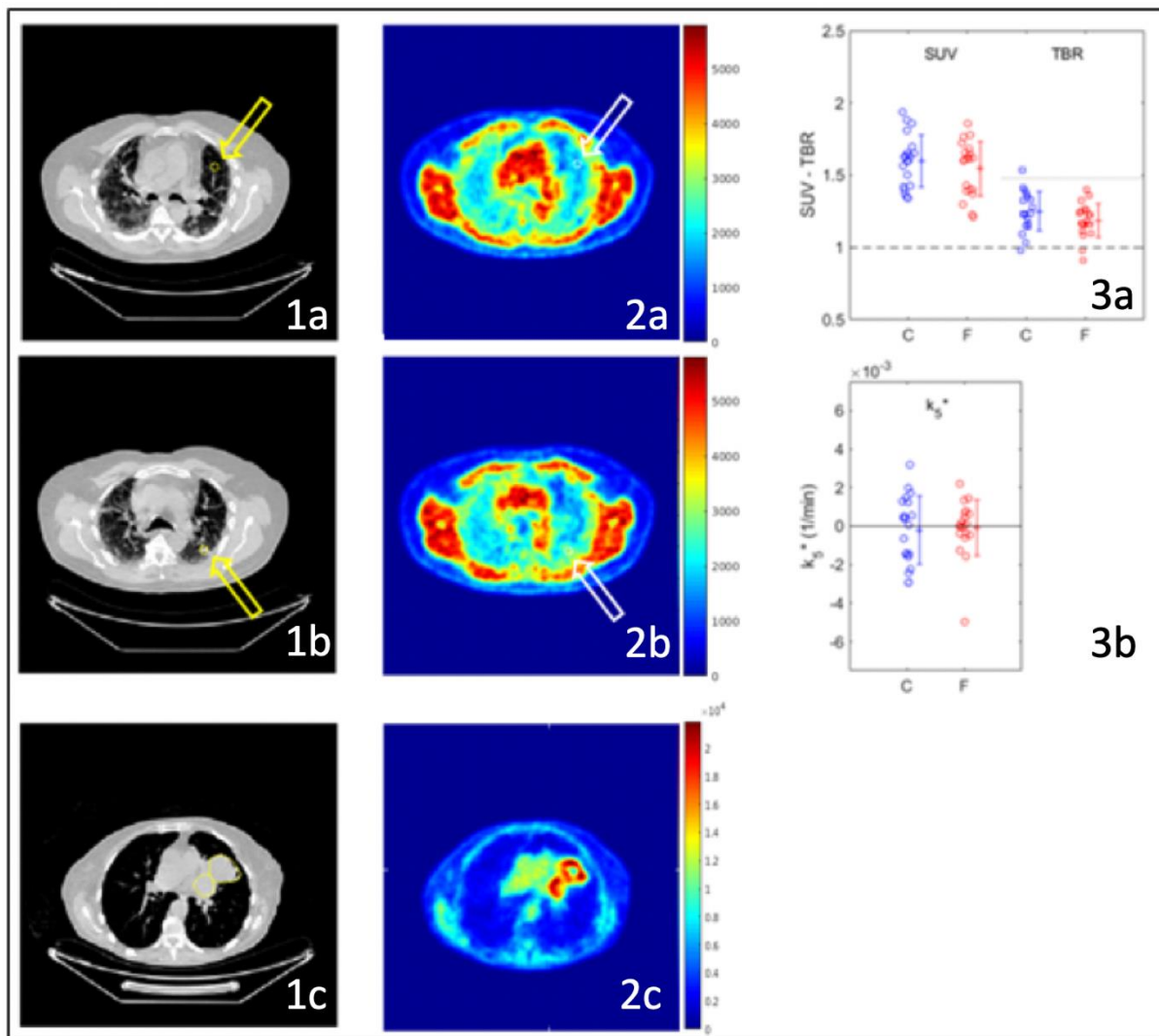
Fig. 1a-1b: CT images of one representative IPF patient, including ROIs for normal appearing (1a) and fibrotic lung tissue (1b);

Fig. 2a-2b: Corresponding ^{18}F-FMISO PET images. (1a-2a and 1b-2b represent different trans-axial planes through the lungs.)

Fig. 3a: SUV_{mean} and TBR_{mean} in normal appearing (C) and fibrotic (F) regions. Error bars show SD. The dotted line indicates a TBR threshold value (see text). 3b: Irreversible trapping rate (k_5^*), derived by a combination of Patlak and compartmental analysis.

Fig. 1c: CT images of a lung adenocarcinoma patient, with corresponding ^{18}F-FMISO PET images (2c; note different scale from 2a-b for PET intensity). There is a high intensity in the tumour due to irreversible trapping of ^{18}F-FMISO in hypoxic tissue.